Point-to-point underwater acoustic communications using spread-spectrum passive phase conjugation

Paul Hursky,[a] Michael B. Porter, and Martin Siderius
Heat, Light, and Sound Research Inc., 12730 High Bluff Drive, San Diego, California 92130

Vincent K. McDonald
Space and Naval Warfare Systems Center, San Diego, 53560 Hull Street, San Diego, California 92152-5001

(Received 13 December 2005; revised 19 April 2006; accepted 19 April 2006)

The ocean is often a complex multipath channel and progress has been made in developing equalization algorithms to overcome this. Unfortunately, many of these algorithms are computationally demanding and not as power-efficient as one would like; in many applications it may be better to trade bit rate for longer operational life. In 2000 the U.S. Navy was developing an underwater wireless acoustic network called Seaweb, for which a number of modulation schemes were being tested in a series of SignalEx experiments. This paper discusses two modulation schemes and associated receiver algorithms that were developed and tested for Seaweb applications. These receiver designs take advantage of time reversal (phase conjugation) and properties of spread spectrum sequences known as Gold sequences. Furthermore, they are much less complex than receivers using adaptive equalizers. This paper will present results of testing these signaling and receiver concepts during two experiments at sea. © *2006 Acoustical Society of America.*
[DOI: 10.1121/1.2203602]

PACS number(s): 43.60.Tj, 43.60.Dh, 43.30.Re [EJS] Pages: 247–257

I. INTRODUCTION

Acoustic signaling for wireless digital communications in the undersea environment can be a very attractive alternative to both radio telemetry systems (vulnerable to weather, rough seas, and pilfering) and cabled systems (vulnerable to commercial trawling). However, time-varying multipath and often harsh ambient noise conditions characterize the underwater acoustic channel, often making acoustic communications challenging. Much effort has been directed at developing channel equalizers and adaptive spatial processing techniques so that coherent phase modulation can be used to achieve the desired high spectral efficiencies.[1,2] These techniques are computationally demanding with many parameters needing to be set, requirements that are not especially well suited for applications where autonomy, adaptability, and long-life battery operation are being contemplated.

Time reversal (or phase conjugation, in the frequency domain) was demonstrated[3–5] in the early 1960s as a means of refocusing sound that had been spread in time by propagation through the ocean. More recent work on this concept[6–8] has seen further experimental validation and the development of a number of applications. In particular, passive phase conjugation can be used for pulse compression,[6] using a vertical line array receiver so that both spatial as well as temporal focusing is achieved, which addresses the difficulties posed by multipath for acoustic communications.[9,10]

In 2000, the U.S. Navy was developing an underwater wireless networking system, called Seaweb, using acoustic communications as the physical transport layer.[11] We were tasked to investigate and test a variant of pulse position modulation (PPM) for use as an alternative modulation scheme in this system. In the course of adapting the original PPM scheme to Seaweb, we realized how this modulation technique was connected to evolving work on time reversal (phase-conjugation),[8] and ended up modifying it to better exploit these new techniques for the Seaweb system.[12] Comparing our work to other reported passive phase conjugate methods,[9,10,13] we use a single-element source and a single-element receiver, without relying on an aperture at the source or receiver for spatial focusing. To compensate, we rely upon the gain from despreading direct-sequence spread-spectrum (DSSS) sequences.[14,15] DSSS is a form of code division multiple access or CDMA. As in terrestrial wireless CDMA systems, this modulation scheme can accomodate multiple users if different orthogonal codes are assigned to different users. In addition, using spread-spectrum sequences renders this modulation scheme more difficult to detect[16] for applications where covertness is desired.

We review time reversal and phase conjugation in Sec. II. Section III presents the details of our modulation scheme. In particular, we show how varying the parameters of PPM to increase its spectral efficiency pushes us to smaller alphabets, leading us to abandon PPM in favor of differential phase-shift keying (DPSK), which has the smallest possible alphabet. In Sec. IV, we present the results of testing these modulation techniques and receiver algorithms in several sea experiments.

Previously, work in both terrestrial wireless and underwater acoustics considered a modulation technique called code shift keying[17] or sequence position modulation[18] (both variants of pulse position modulation or PPM) that also uses

[a]Electronic address: paul.hursky@hlsresearch.com

spread-spectrum sequences.[14,15] As we will outline, we favor DPSK over PPM, but we note that code shift keying can potentially benefit from time reversal (phase conjugation) as well. We will also comment on the similarity of our DPSK scheme to a Rake receiver (a type of receiver often used in spread spectrum systems[14]).

II. HOW TIME REVERSAL (PHASE CONJUGATION) BENEFITS ACOUSTIC COMMUNICATIONS

A communication system consists of a transmitter that sends a data-modulated waveform through a channel (in our case, the ocean) and on to a receiver which must perform some processing to recover the transmitted data. Typically, the channel introduces distortion that limits the receiver's ability to recover the transmitted information. This distortion includes attenuation, time spreading or multipath, and Doppler shifts and spreads. The Doppler effects are due to transmitter and receiver motion, as well as the motion of the ocean boundaries and the ocean itself. If time spreading is present in the channel (due to transmitted signals arriving along multiple paths), previously transmitted symbols may corrupt the detection of the current symbol, a problem known as intersymbol interference.

Various receiver algorithms have been developed to despread the multipath arrivals (or equalize them, viewed in the frequency domain). In some cases, the diversity provided by multiple arrivals is exploited so successfully that a net processing gain is achieved, thus turning a problematic channel property into an asset. Reducing intersymbol interference is the "holy grail" of communications, because it enables symbols to be transmitted at very high rates. One approach for coping with intersymbol interference is to use an adaptive filter[19] to adjust a set of filter coefficients to minimize the mean squared difference between the filtered output and either a known training sequence or the closest known discrete symbol value in a "decision-directed" mode.[2] Although fast algorithms for such equalizers have been the subject of much research, this approach still requires great care with respect to computational load, algorithm stability, and automated selection of adaptive filter parameters for an unknown and often time-varying channel.

The time reversal (phase-conjugation) approach that we are exploring in this paper avoids the explicit recovery of the channel and its subsequent equalization via signal processing and its associated algorithmic complexity. Instead, this approach implicitly recombines the multiple arrivals signal instead of trying to invert the channel.[9,10] To review how this focusing is achieved, Fig. 1 illustrates two ways of implementing time reversal, or phase conjugation (its frequency domain equivalent). We have labeled these two configurations active phase conjugation,[7,8] or APC, and passive phase conjugation,[6] or PPC. Both have been experimentally validated in the ocean. The channel impulse response (CIR) function is $h(t)$ and its Fourier transform is $H(\omega)$. $H(\omega)$ is the Green's function for the particular ocean waveguide and source and receiver locations, although we omit the dependence on locations in our notation. Recall that, in the frequency domain, the convolution of $h(t)$ and $s(t)$ is $H(\omega)S(\omega)$.

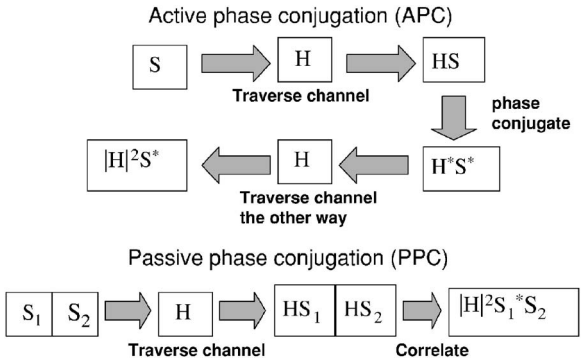

FIG. 1. Active and passive phase conjugation.

Similarly, the correlation of $s_1(t)$ and $s_2(t)$ is $S_1(\omega)S_2^*(\omega)$, where the asterisk indicates complex conjugation. In Fig. 1 and the text below, we use the frequency domain equivalents of all waveforms, and drop the dependence on ω.

In the active configuration (APC):

- The left-hand station transmits a waveform S, which travels through the channel H (from left to right in Fig. 1), and is recorded on the right-hand station as HS.
- The right-hand station time reverses the received waveform, or equivalently, phase conjugates it, producing H^*S^*, and retransmits it back to the left-hand station (from right to left in Fig. 1). The retransmitted waveform can carry either a sign or a phase to convey information (back) to the left-hand station. Assuming the channel has not changed, the time-reversed waveform H^*S^* travels back through the same channel, and is convolved with H again, producing $|H|^2S^*$ at the original left-hand station, the time-reversed version of the original signal S convolved with the autocorrelation of H. The left-hand station is the information receiver in this configuration.

In the passive configuration (PPC), shown in the lower part of Fig. 1:

- The left-hand station transmits S_1, which travels through the channel H, and is observed on the right-hand station as HS_1.
- The left-hand station transmits S_2, which is observed on the right-hand station as HS_2 (again, if the channel has not changed).
- The right-hand station cross-correlates HS_1 and HS_2, producing $|H|^2S_1S_2^*$, the correlation of S_1 and S_2, convolved with the autocorrelation of the CIR H. The right-hand station is the information receiver in this configuration.

The basic idea in phase conjugation is that the autocorrelation of the CIR $|H|^2$ tends to reconcentrate or focus the multipath arrivals at zero time lag. The term $|H|^2$ is the time reversal or phase conjugation focusing operator.[20] However, depending on the distribution of the multipath arrivals in $h(t)$, the autocorrelation may also have temporal sidelobes that result in residual intersymbol interference, even after focusing. Other researchers[9,21] have used arrays of receivers

or transmitters to average down these temporal sidelobes. The different transmitter-receiver focused terms (i.e., $|H|^2S$ or $|H|^2S_1S_2^*$, depending on the configuration) are typically aligned along their main peak, prior to averaging. As a result, they share a common main peak, but have sidelobes at different locations. Upon averaging, all elements contribute to the same main peak, but spread their sidelobes wherever they may fall.

In our technique, we avoid the cost and complexity of transmit or receive arrays by using spread spectrum sequences. This relies upon despreading gain and temporal focusing alone,[12] although this does not yield bit rates as high as can be produced with source and receiver arrays. This focusing, or multipath recombination, is achieved at each "symbol" by forming an inner product of the current and predecessor snapshots of the channel, where each channel snapshot is the output of a correlator matched to the known spread spectrum sequence (we cycle through a known set of orthogonal sequences). Such a receiver structure is similar in function to and has the (low) computational complexity of a linear equalizer,[19] although it is approximating the channel inverse by its adjoint (our receiver forms the inner product of H and its adjoint H^*, to form the focusing operator $|H|^2$).

Figure 1 shows that the APC configuration focuses the original waveform S (producing $|H|^2S$ at its receiver station), while the PPC configuration focuses $S_1S_2^*$ (producing $|H|^2S_1S_2^*$ at its receiver station), the correlation of the two consecutively transmitted waveforms (S_1 and S_2). Therefore, in our PPC configuration, the message must be encoded in the correlation of the two consecutively transmitted waveforms S_1 and S_2. Encoding information in the correlation of two waveforms is not a typical signaling scheme and may provide some advantages, although we have not been particularly creative in pursuing this, other than to try the simple variations described below.

III. WAVEFORM DESIGN FOR POINT-TO-POINT ACOUSTIC COMMUNICATIONS USING PASSIVE PHASE CONJUGATION

We will describe two signaling schemes, one based on pulse position modulation (PPM), the other on differential phase shift keying (DPSK).[19] We have implemented these two modulation schemes to take advantage of passive phase conjugation (the PPC configuration in Fig. 1). These waveform designs rely upon transmitting two waveforms, s_1 and s_2, in which information bits have been embedded, with the expectation that both s_1 and s_2 will propagate through the same channel h, so that they are received as HS_1 and HS_2 (in the transform domain). As discussed in the previous section, the passive phase conjugation (PPC) is realized by correlating these received waveforms to produce $|H|^2S_1S_2^*$. This operation produces a despread or focused $S_1S_2^*$ because $|H|^2$ combines the multipath arrivals.

As already mentioned in Sec. II, because we are working with single hydrophones (no arrays), we have more of an intersymbol interference problem than in configurations where arrays are used. To compensate for this, we rely upon families of sequences called Gold codes,[14,15] designed to minimize the correlation between the sequences in each family. Gold codes are similar to maximal-length sequences, or m-sequences, that are often used in the underwater acoustic community for their autocorrelation properties.[22,23] Gold sequences, like m-sequences, are bipolar sequences with values -1 and 1. Their special property is that any two different Gold sequences from the same family have very low (circular) cross-correlation values (i.e., at all lags). For integers $m>2$ at which a *preferred pair of m-sequences* can be found, a family of Gold sequences can be derived whose cross-correlation spectrum is three-valued. There are $2^{m-1}+2$ Gold sequences in each family. When transmitted, each Gold sequence modulates the phase of a carrier (i.e., using binary phase-shift keying or BPSK modulation).

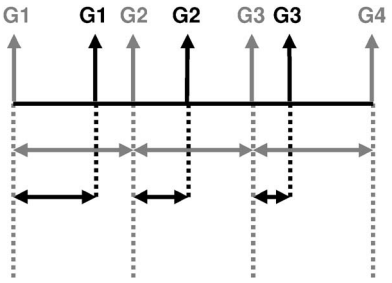

FIG. 2. This diagram illustrates the waveform design for PPC-PPM. Each arrow indicates the onset (in time) of a Gold sequence. Each G_i indicates that the ith Gold sequence is being used (from a particular family of sequences). Each symbol consists of a gray reference pulse and a black position pulse (so three symbols are shown above). The information is conveyed by the separation between the reference pulse and the position pulse (shown by the horizontal black arrows). All sequences have the same length—the interval between consecutive reference pulses (shown by the horizontal gray arrows). Gold sequences corresponding to the position pulses of consecutive symbols may overlap.

Our modulation cycles through a series of Gold sequences (i.e., from the same family), using a different Gold sequence for each symbol. The particular order of the Gold sequences being transmitted is known at the receiver, so the appropriate matched filter can be applied to each received symbol. When symbols overlap due to multipath, the low cross-correlation property of the Gold sequences ensures that the different matched filters do not let through much of the interfering symbols. To accomodate multiple users simultaneously, different subsets of Gold sequences can be assigned to different users—each user must have enough sequences so that the time it takes to cycle through this user's subset exceeds the time spreading in the channel. However, note that we do not fully exploit the touted low cross-correlation property of these sequences, because in the presence of multipath, the correlation that is being performed on all the different multipath arrivals is not circular.

A. Pulse position modulation using Gold sequences (PPC-PPM)

Figure 2 shows how we implement (PPM) to take advantage of passive phase conjugation (PPC). Here G_i indicates the ith Gold sequence from a family of 2^m+1 sequences, each a sequence of 2^m-1 bipolar symbols, or chips, where the start of each sequence is indicated by a single arrow. Arrows indicating the onset of each Gold sequence rather than the full-length sequences are shown to illustrate

the scheme. Each sequence is actually a bipolar sequence modulated by a carrier (i.e., BPSK modulated) of length indicated by the horizontal gray arrows. Each G_i is repeated, with the first G_i (indicated in gray) setting a reference position, relative to which the position of the second G_i (indicated in black) is measured. The varying distances between reference and second positions are indicated by the horizontal black arrows. The position of the second G_i is purposely varied to convey the information bits being transmitted, hence the name PPM. If the time interval between reference G_i's, indicated by the horizontal gray arrows, from G_i to G_{i+i}, is divided into N resolvable time slots, each pair of G_i's will carry $\log_2 N$ bits of information. To relate this design to the notation in the introduction above, s_2 is identical to s_1, but they overlap and the time between them is varied to set the pulse position.

At the receiver, a matched filter tuned to G_i performs a pulse compression on each G_i and reproduces the multipath arrival structure associated with both instances of G_i. The arrivals associated with G_j (j not equal to i) are to a large extent suppressed (by the matched filter tuned to G_i), since the different Gold sequences have low cross correlation. After this pulse compression, the matched filter output contains two copies of the CIR, overlapped and delayed with respect to one another, corresponding to each of the two G_j. At this point it is possible to decode the information from the relative positions of the dominant arrivals only, but this would not take advantage of the additional signal energy available in the other arrivals. Instead, the concept is applied to our pulse-compressed pair of G_i receptions. Each is spread by what is probably the same channel, since there has been little time for the channel to have changed during this interval, so if we auto-correlate the matched filter output (tuned to G_i), we implicitly autocorrelate the CIR H by which each of the two G_i receptions have been spread, realizing a filter consisting of the time reversal (phase conjugation) operator $|H|^2$ as discussed in the previous section.

It is interesting to note that this refocusing could also be exploited in the code shift keying work, if a reference sequence and a sequence to indicate position were somehow incorporated [we need to correlate two copies of the $h(t)$ to form the autocorrelation of $h(t)$ which provides the focusing]. Our modulation scheme differs from those described in the code shift keying and sequence position modulation work,[16,18] in that we do not circularly permute the waveform that sets the position (for PPM), but instead merely delay it.

B. Differential phase shift keying (DPSK) using Gold sequences (PPC-DPSK)

With a bandwidth B, we can resolve PPM time slots spaced at intervals of $1/B$. A symbol period of T seconds will have room for BT time slots (or positions), or $\log_2 BT$ bits per symbol, with a bit rate of $\frac{\log_2 BT}{T}$. The bit rate can be increased by increasing B or reducing T. Because the denominator T grows faster than numerator $\log_2 T$, increasing the number of PPM slots by lengthening T actually reduces the bit rate. So, although we were originally motivated to use PPM to pack more bits into each symbol, we find instead that

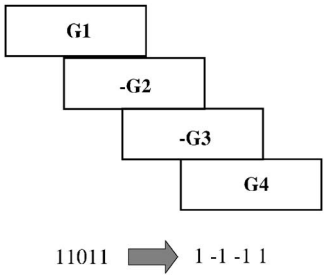

FIG. 3. PPC-DPSK waveform design.

reducing the number of PPM slots is what increases the bit rate. Ultimately, if we want a maximum bit rate, we should use the smallest number of PPM slots that we can, which suggests an alphabet of size two. In this section, we back off from using PPM entirely, and adopt a DPSK framework, encoding our information bits in the relative polarity of neighboring Gold sequences.

Figure 3 shows an alternative PPC modulation waveform design. In this case, we cycle through the 2^m+1 Gold sequences, spacing them at regular intervals, but varying their sign. The transmitted information is recovered at the receiver by comparing the sign of the current G_i with the sign of its predecessor G_{i-1}, in effect realizing a DPSK modulation. In this case, s_1 and s_2 are different Gold sequences, G_{i-1} and G_i, with the relative polarity indicating the information bit being transmitted.

Figure 4 shows how each pair of consecutively transmitted Gold sequences, G_i and G_{i-1}, are processed. S_1 and S_2 are the waveforms at the receiver corresponding to G_{i-1} and G_i, with S_2 following immediately after S_1. At the transmitter, a sign change may be applied to either G_{i-1} and/or G_i, depending on the information bit being transmitted. It is this relative sign that carries the information, and which must be recovered by the receiver. After traveling through the channel, S_1 is HG_{i-1} and S_2 is HG_i, each with a possible information bearing sign change. S_1 and S_2 overlap and their start times are calculated by a symbol timing process (to be described later). At the receiver, a matched filter tuned to the appropriate Gold sequence (G_{i-1} for S_1 and G_i for S_2) is applied to each of the two waveforms, producing $H|G_{i-1}|^2\text{sign}(G_{i-1})$ and $H|G_i|^2\text{sign}(G_i)$. The $|G|^2$ factors are pulse compressions of the Gold sequences. Both of these matched filter outputs are essentially estimates of the channel H with the polarity originally applied at the transmitter to carry the information

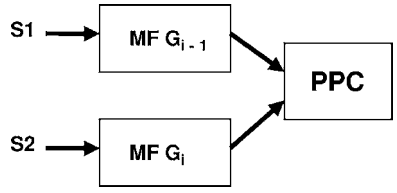

FIG. 4. This is the PPC-DPSK receiver design, in which every pair of consecutively arriving signals S_1 and S_2 is processed by a pair of matched filters, S_1 being correlated with Gold sequence G_{i-1}, and S_2 being correlated with Gold sequence G_i. The two matched filter outputs are correlated (in block PPC) to compare the phases of S_1 and S_2. It is the phase difference between S_1 and S_2 that carries the information bit. We have only tested phase differences of 180 deg (i.e., changing the sign of S_2 relative to S_1 or not).

bit. Although we could compare the signs of individual peaks from the two channel estimates, we want to combine all of the multipath arrivals before we do that. As in the PPC-PPM modulation, we correlate the two matched filter outputs, producing waveform proportional to $|H|^2, |G_{i-1}|^2, |G_i|^2$, and the product of the signs of the two transmitted waveforms. Again, we end up filtering our information bearing waveform, in this case $\text{sign}(G_{i-1})\text{sign}(G_i)$, by the time reversal (phase conjugation) focusing operator $|H|^2$. This implicitly recombines the multipath. The information bit is recovered from the sign of this final correlation.

The PPC-DPSK modulation scheme is similar to spread-spectrum schemes that use a Rake receiver for recombining multipath arrivals.[24] In both cases, a matched filter is applied to a spreading sequence to isolate multipath arrivals. In the case of a Rake receiver, multiple matched filters are applied at a number of delays, or "fingers" (of the Rake), prior to combining the contributions from each "finger" so that they are all aligned in time. In our PPC-DPSK, phase conjugation or the inner product of $H|G_{i-1}|^2\text{sign}(G_{i-1})$ and conj $[H|G_i|^2\text{sign}(G_i)]$ is used to focus the multipath arrivals (this inner product contains the focusing operator $|H|^2$). In the case of the Rake receiver, some decision must be made as to where to position the multiple "fingers" of the Rake receiver. In Sec. IV B, we will show how we have borrowed an idea from the Rake receiver to greatly improve our demodulation results for the PPC-DPSK scheme.

C. Discussion

The usual dilemma in APC and PPC, at least in how it has been implemented previously, is that the channel estimate must be periodically refreshed to keep up with a time-varying channel. This is done by interrupting the flow of information bits to send a probe pulse to recalibrate the channel and waiting for the channel to clear before reinitiating information bits. An alternative to "clearing the channel" in this way has been investigated by other authors,[13] in which the channel estimate is continually refreshed, using the current block of detected symbols to estimate the channel for the next block of symbols. The channel is estimated by finding the best fit (in a least-squares sense) to the received data and the decoded symbols, although this seems to get away from the minimalist implementation that is usually cited as PPC's main attraction. Our two transmission schemes (PPC-PPM and PPC-DPSK), described in the previous section, do not require an explicit channel estimate since they implicitly refresh the channel state information by cross-correlating waveforms corresponding to consecutive pulses (PPM) or symbols (DPSK).[12]

The spacing between consecutive sequences determines the bit rate

$$R = 1/T_{\text{spacing}} \tag{1}$$

but we cannot reduce this spacing indiscriminately, because these sequences are not perfectly orthogonal, especially after being convolved with a CIR function. Their touted good (i.e., low) cross correlation properties are based upon periodic (or circular) cross correlation and accurate "framing" of the sequence. Neither condition is realized in our modulation schemes, because the various multipaths arrive at different times and because the different sequences are staggered in our modulation scheme. As a result, there is more interference between the overlapped sequences than is predicted for these sequences under perfect conditions. Increasing the bit rate by reducing the symbol spacing creates more overlap between sequences and makes the interference worse.

Gold sequences have lengths of 2^m-1 for a particular choice of m. The longer the sequence, the lower its autocorrelation sidelobes and correlations with other Gold sequences from the same family. However, longer sequence lengths mean more of an overlap with following sequences, if the spacing is kept the same. As a result, the length must be chosen as a compromise between these two competing considerations.

The chip rate should ideally be matched to the bandwidth. A chip rate of 4 kHz results in spectral nulls at the edges of our 8 kHz band, and is thus optimal for our bandwidth. We also tested chip rates of 8 and 16 kHz in order to gain their resulting higher bit rates, knowing they are not matched to our 8–16 kHz band and that their cross-correlation properties would be degraded as a result of losing out-of-band information.

When consecutive Gold sequences are overlapped, an unacceptably high peak to average power ratio can result, as in multiple carrier modulation schemes, such as orthogonal frequency-division multiplexing or OFDM. A set of constructively interfering Gold sequences can produce an unusually large and isolated peak. If we scale the transmitted waveform according to this single isolated peak, our transmitted waveform will have an unacceptably high peak-to-average-power ratio, resulting in very low average transmitted power. To avoid this, we clipped isolated peaks to minimize this loss in transmitted power, recognizing that this results in some degradation in the receiver matched filter, since some of the transmitted waveform was lost to this clipping. The incidence of unusually large and isolated peaks is proportional to the number of overlapping Gold sequences, so this too limits our bit rates.

IV. RESULTS OF TESTING DURING SIGNALEX EXPERIMENTS

The U.S. Navy has supported a series of sea tests under the SignalEx program[25] to measure channel effects upon different underwater acoustic signaling schemes, including our passive phase conjugate technique. These tests have been performed in a variety of environments using lightweight, modular hardware units, called Telesonar Testbeds, shown in Fig. 5. These testbeds, developed at SPAWAR Systems Center, are unique, high-fidelity, modular, reconfigurable, autonomous, wide-band instruments for high-frequency acoustic propagation and communication research. They consist of a PC-104, single-board computer in a deployable bottle, including hard drives for recording received waveforms or sourcing waveforms for transmission. The testbed can record waveforms on a four-channel receive array (spaced for diversity, with elements separated by five wavelengths at 12 kHz) and transmit in three bands, 8–16, 14–22, 25–50 kHz. A very

FIG. 5. Telesonar Testbed used to collect data.

accurate clock allows for time-division multiplexed transmissions from multiple testbeds. The testbed units are also equipped with a commercial acoustic modem for status checking and remote control. During a typical experiment, two testbed units are deployed. One is moored to the sea floor and the other is deployed over the side of a small boat, which is either anchored or allowed to drift. One testbed transmits a preprogammed sequence of waveforms stored on disk, and the other testbed records the received waveforms (to disk), after they have traveled through the ocean waveguide. The transmission sequences and power levels can be controlled remotely via the commercial modem. We will present results for fixed-drifting configurations at two sites.

A. Results from SignalEx-E: Ship Island, off Gulfport during AUV/Modem Fest 2001

The SignalEx-E experiment was performed near Ship Island on 24-25 October 2001, during ModemFest/AUVFest off the coast of Florida. The source was deployed at a depth of roughly 2 m over the side of a boat that was allowed to drift at roughly 0.6 m/s. The receiver was moored to the sea floor. The bathymetry along the transmission path was nearly constant at a depth of 5 m. Figure 6 shows the drift track, starting at a range of about 1 km and ending at a range of roughly 5 km.

Figure 7 shows the CIR measured by applying a matched filter to a series of hyperbolic frequency-modulated (HFM) chirps, each 50 ms long, sweeping from 8 to 16 kHz, transmitted every 250 ms. There is virtually no multipath in this extremely shallow water channel (the horizontal axis spans only 6 ms). The bottom was silt (from examining the receiver moorings), but even if it were more reflective, acoustic paths having even a slight grazing angle would interact with it so many times over the ranges we were operating at that they would be absorbed. The few bottom-interacting paths that would get through at very shallow grazing angles would have virtually the same travel time as a direct or surface reflected path (and would contribute to the response shown in Fig. 7).

Both the PPC-PPM and PPC-DPSK modulation schemes were tested at this site, each at two different rates. The transmitted packets for each of these rates were roughly 15 s long.

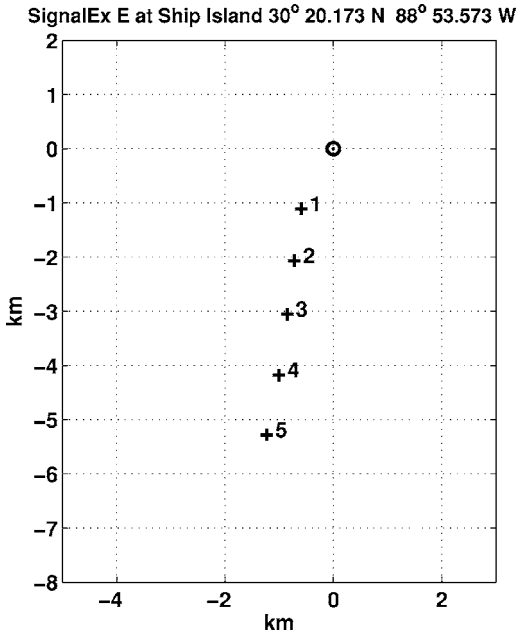

FIG. 6. SignalEx E configuration by Ship Island near Gulfport during AUV/Modem Fest 2001, showing the receive Telesonar Testbed at the origin, and five locations of the transmitter during its drift away from the receiver, when our packets were transmitted.

The PPC-PPM modulation used $m=7$ Gold sequences, each Gold sequence being repeated, as discussed in Sec. III A. Rates of 126 and 188 bps were tested. The lower-rate modulation used Gold sequences with a chip rate of 4 kHz and 4 bits per PPM symbol (16 PPM slots). The higher-rate modulation used Gold sequences with a chip rate of 8 kHz with 3 bits per PPM symbol (8 PPM slots).

The PPC-DPSK modulation used $m=7$ Gold sequences with a chip rate of 8 kHz (i.e., 8000 sequence bits per second). Rates of 160 and 264 bps were tested by varying the symbol periods (i.e., the spacing between sequences, or equivalently, between DPSK symbols).

Figure 8 shows a diagnostic output of our modem at the

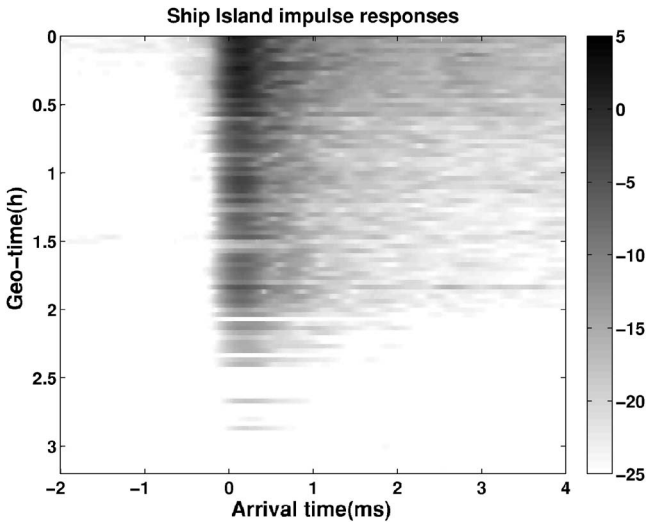

FIG. 7. Channel impulse response (CIR) measured as the transmitter drifted away from the receiver during SignalEx E at Ship Island near Gulfport, during ModemFest 2001.

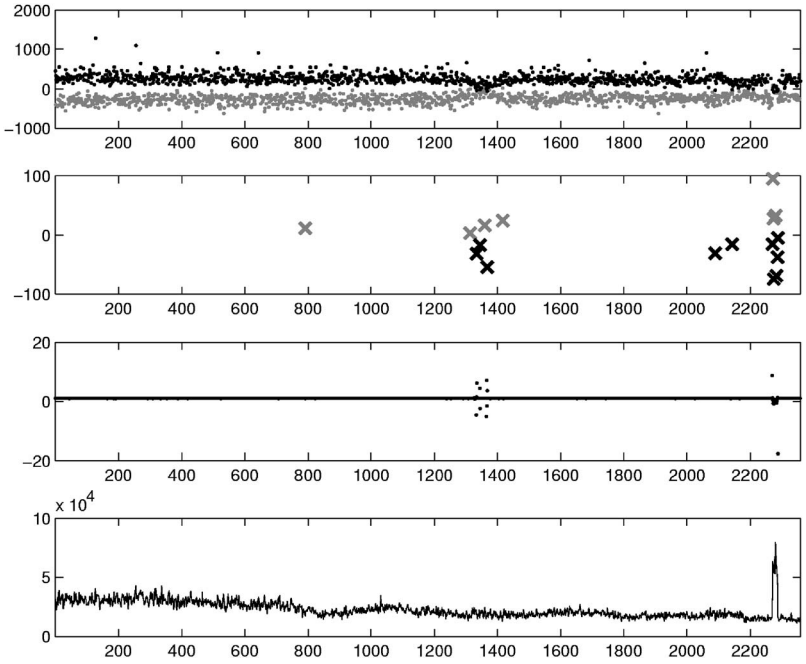

FIG. 8. Diagnostic display from testing the 264 bps PPC-DPSK modulation at 5 km range. All four plots are synchronized along a common x axis that shows the 2359 symbols that make up the packet. The first plot shows values for all the symbols in the packet (the sign of these values is used to "detect" which information bit was transmitted). The second plot shows only the symbols that were incorrectly labeled (note the different y-axis scale, compared to the first plot). The third plot shows deviations of estimated symbol times from expected symbol times (the symbol timing errors near the middle of the packet coincide with the first group of bit errors). The fourth plot shows the matched filter energy output by the symbol timing calculation (the energy spike near the end of the packet coincides with another group of bit errors).

5.4 km range for the 160 bps PPC-DPSK transmissions. This is the packet at which the most bit errors were observed. All four plots are synchronized along a common x axis that indicates symbol number. The upper two plots show symbol values over the length of a 2359 bit packet (i.e., values of $|H|^2 S_1 S_2^*$ from Sec. I), with the first plot showing values for *all* the symbols in the packet, and the second plot showing only the values at which bit errors occurred. The third plot shows the deviations of the estimated symbol times from symbol times calculated by adding the known symbol period to the previous symbol time. The purpose of this plot is to identify which bit errors are due to symbol timing errors. In this case, symbol synchronization loss accounts for some of the bit errors near the middle of the packet. The fourth plot shows the matched filter energy from the symbol timing calculation, and is intended to identify when bit errors are caused by low SNR. In this case, there is an energy spike near the end of the packet, caused by a loud broadband transient of unknown origin (that is apparent in the spectrogram of this data). The errors that occur at this time are probably due to this transient. The separation between positive and negative symbol values in the first plot is also a good indicator of the quality of the information bits being detected. When this gap closes, there is not much signal excess for ambient noise to overcome to cause a bit error.

Table I summarizes the results of testing the PPC-DPSK and PPC-PPM schemes.

B. Results from SignalEx-F: off the coast of La Jolla in San Diego, California

Figure 9 shows the bathymetry and drift track (top plot) and the sound speed, source, and receiver depths, and the bottom composition (bottom plot) from the SignalEx-F test performed off the coast of La Jolla in San Diego, California, on May 10, 2002.

Figure 10 shows how the ocean channel varied with range (from about 500 m to 6 km) as the source platform drifted away from the receive platform over a five hour time interval. Each scan line is the result of averaging the matched filter outputs from forty 50-ms chirps, repeated at 250 ms intervals. The matched filter outputs were aligned by circularly shifting each scan line relative to its predecessor, so that the maximum correlation of each two consecutive scan lines is shifted to time lag zero.

A set of PPC-DPSK packets, one at each of the three rates being tested, was transmitted every half hour during this test. Each packet contained 2240 bits. Each data packet was preceded by a 100–ms LFM chirp sweeping from 8 to 16 kHz, which was used to determine the start of a packet (i.e. initial synchronization).

We transmitted 127-chip Gold sequences ($m=7$) in the 8–16 kHz band at chip rates of 4, 8, and 16 kHz (having lengths of 32, 16, and 8 ms), spaced at intervals of 12, 6, and 3 ms (for rates of 80, 160, and 320 bps). There are 129 Gold sequences at $m=7$, so unless the channel spread is exceptionally long (387 ms for the 3 ms spacing), there are enough sequences to ensure that cycling through them will not result in a situation where a previous transmission of a particular sequence interferes with a current transmission of that same sequence, due to the channel spread.

TABLE I. Bit error rates from PPC-DPSK and PPC-PPM modulation schemes during SignalEx-E (at Ship Island) at five transmitter-receiver ranges (see Fig. 6).

	DPSK-1	DPSK-2	PPM-1	PPM-2
Range(km)	160 (%)bps	264 (%)bps	126 (%)bps	188 (%) bps
1.2	0.0	0.7	0.4	7.0
2.2	0.0	0.5	0.6	2.0
3.2	0.4	1.3	1.4	3.0
4.3	0.0	3.0	0.7	5.0
5.4	0.8	9.3	3.1	Synch failed
	2359 bits/ packet	3899 bits/ packet	1880 bits/ packet	2790 bits/ packet

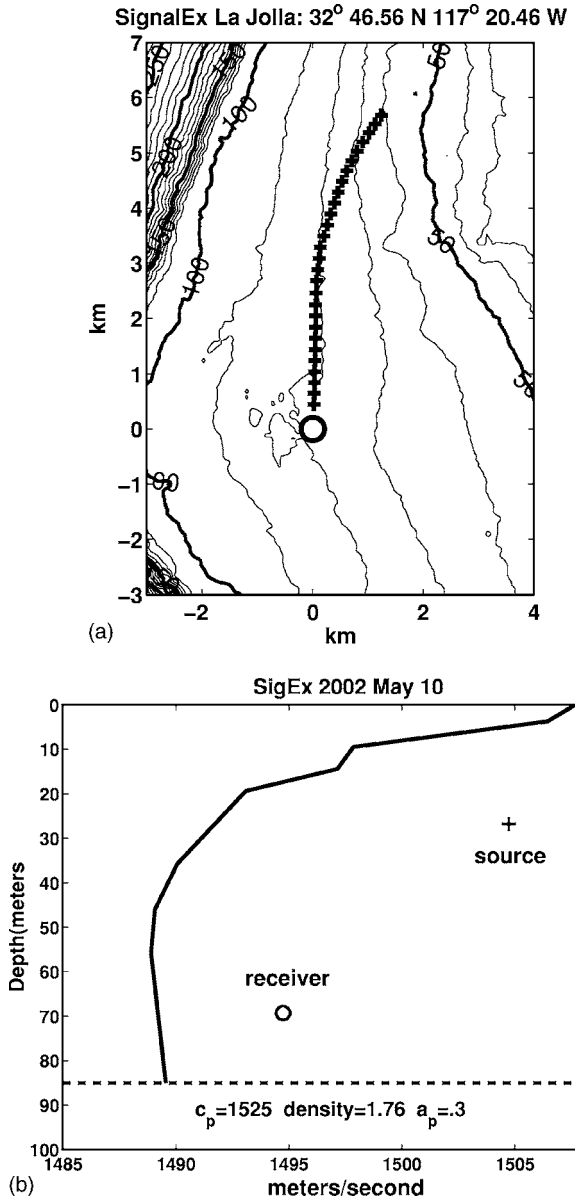

FIG. 9. The top plot shows the SignalEx F configuration in La Jolla, 2002, with the fixed receiver at the origin, and a series of transmitter locations (indicated by plus markers) as the source platform drifted away from the receiver. The bottom plot shows the source and receiver depths, the sound speed profile, and the bottom properties. (a) Bathymetry contours and source track. (b) Sound speed profile and bottom properties.

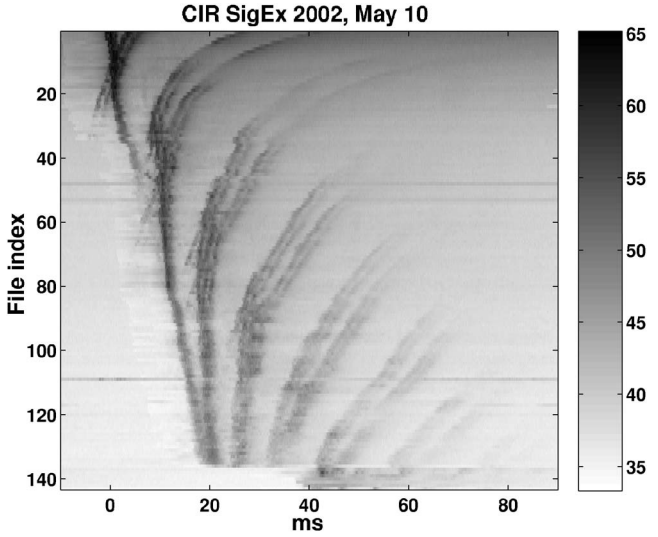

FIG. 10. Channel impulse response (CIR) measured during SignalEx F (off La Jolla in San Diego, CA, in 2002), using dedicated LFM channel probes. This shows how the CIR varies as a function of range (from 500 m to 6 km). These channel measurements correspond to periodic probe pulse transmissions (every two minutes) as the source platform drifted away from the receiver.

This data was initially processed using the PPC receiver described above, but showed poor results in this channel, compared to previous tests and other modulation schemes [CDMA with a Rake receiver and Multi-frequency shift keying or MFSK]. After reviewing the data in great detail, we modified the receiver algorithm to threshold the matched filter outputs, so that contributions whose values were less than 25% the value of the tallest peak were discarded. Only the values exceeding this 25% threshold were used to calculate the polarity of each symbol relative to its predecessor.

Apparently, due to the greater multipath in this environment, the contribution from the sidelobes of the Gold sequence auto and cross correlations and of the CIR autocorrelations was overwhelming the information in the multipath arrivals. This is not surprising, given that we were (1) pushing the chip rate to 8 and 16 kHz, twice and four times the 4 kHz chip rate supported by our 8–16 kHz band and (2) overlapping the Gold sequences to increase the information bit rate. Thresholding the matched filter outputs so that only the high amplitude multipath arrivals were "counted" resulted in greatly improved bit error rates.

This idea is also used in Rake receivers for modulation schemes, where contributions from Rake "fingers" are also thresholded and only the higher amplitude contributions are used to form the detection statistic.[24]

Figure 11 shows various diagnostic displays from our PPC-DPSK receiver for the 160 bps rate at 1.8 km range (packet 3). The upper left plot shows the CIR measured from a 100 ms LFM chirp, used as a synchronization marker roughly 30 ms ahead of the information bits. The upper right plot, a gray scale image, shows channel measurements made using the information-carrying Gold sequences. Each column of this image contains a channel estimate, with multipath time of arrival in milliseconds along the y axis, and symbol time (slow time) in seconds along the x axis. Each Gold sequence is roughly 16 ms long, and overlaps its immediate predecessor by 10 ms and its earlier predecessor by 4 ms, since the sequences are transmitted every 6 ms. The low cross correlation between different Gold sequences minimizes the "cross talk" between consecutive, overlapping Gold sequences, and provides frequent channel measurement updates (every 6 ms). The lower left plot looks very similar to the previous plot (upper right), but it is a black and white dot plot, with the dots indicating the subset of CIR waveform samples that were used to calculate the phase difference for each two consecutive Gold sequences (i.e., for PPC-DPSK). The same strong multipath arrival pattern is visible in both the upper right image and the lower left dot plot. The dots correspond to those samples whose values exceed the 25%

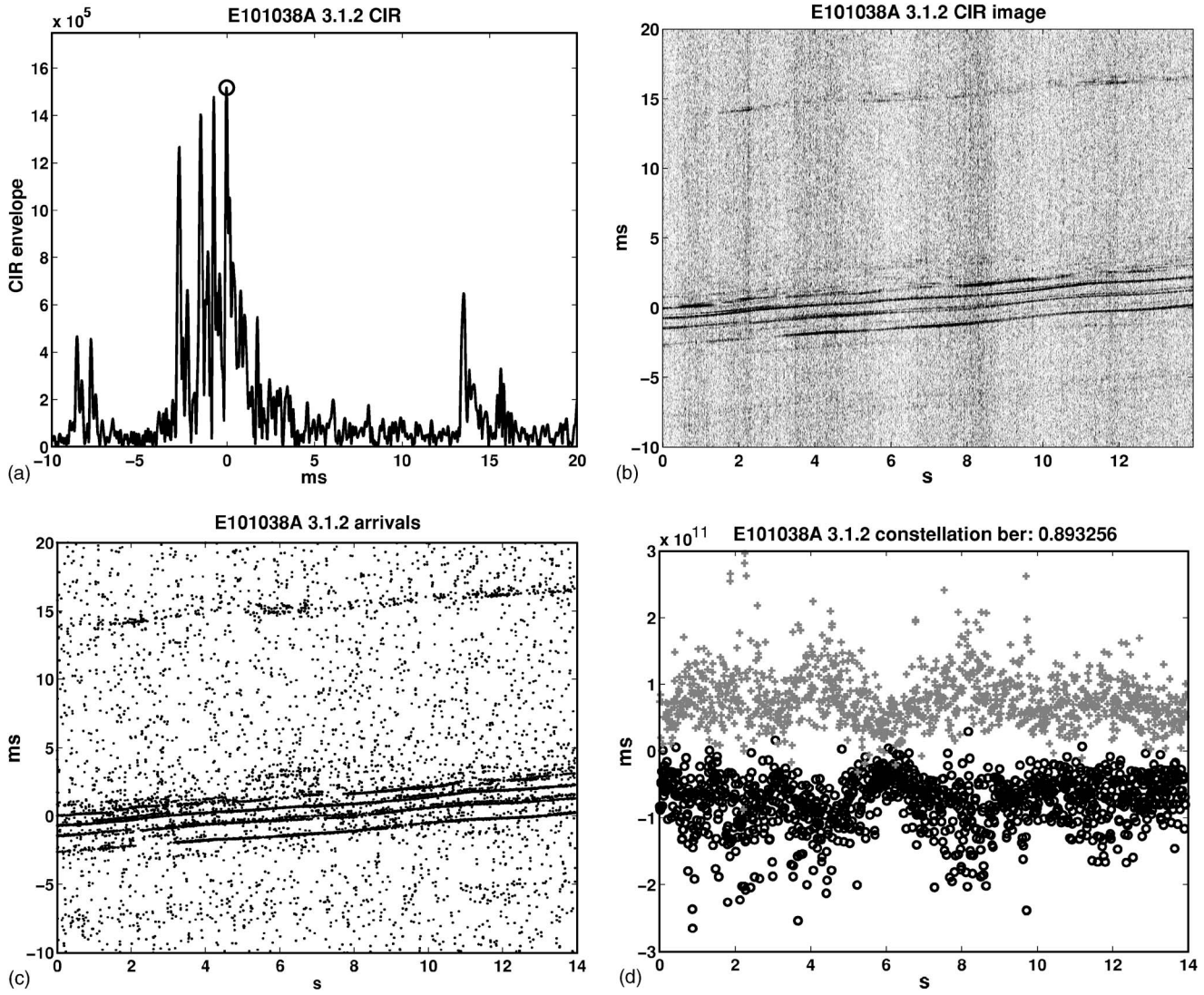

FIG. 11. Measured channel impulse response (upper left), gray-scale image of channel measurements using Gold sequences (upper right), dot plot showing subset of samples that exceed the 25% threshold (lower left), and constellation from the 160 bps packet 3 (lower right). (a) Initial measurement of channel impulse response (from probe). (b) Channel measurements, one per symbol, made from Gold sequences. (c) Multipath arrivals detected from the envelope of matched filter output (on each Gold sequence). Each dot indicates a sample used to form the symbol detection statistic. (d) DPSK constellation versus time.

threshold set relative to the tallest peak in each channel estimate. The lower right plot shows the PPC-DPSK constellation values for the entire 14 s packet.

Table II summarizes the results of testing our PPC-DPSK modulation scheme at three different rates during the SignalEx F experiment. The uncoded error rates for both the 80 and 160 bps data sets were low enough that a convolutional decoder could completely recover the data without errors. However, the bit error rates observed for the 320 bps rate were probably catastrophic at all ranges.

V. SUMMARY AND CONCLUSIONS

PPC implicitly equalizes the channel by refocusing channel spread. We have shown how PPC temporal compression, in a point-to-point configuration (i.e., without arrays of sources or receivers), can be augmented by using Gold sequences to implement receivers based on both PPM and DPSK modulation schemes. We have shown that the PPC-DPSK modulation is more spectrally efficient than PPC-PPM. These PPC-based modulations and their associated receiver algorithms were tested at two SignalEx experiments, one at Ship Island, Mississippi, a very shallow water site with a depth of 5 m and very little channel spread (both PPC-PPM and PPC-DPSK were tested there), and another off La Jolla, California, a moderately shallow water site with a depth of 75 m and moderate channel spread (only PPC-DPSK was tested there). For PPC-PPM, bit rates of 126 and 188 bps were reliably demodulated at the Ship Island site (reliable meaning uncoded bit error rates were low enough that a convolutional decoder would be able to completely recover from them). For PPC-DPSK, bit rates of 160 and 264 bps at Ship Island, and bit rates of 80 and 160 bps at the La Jolla site, all in a 8–16 kHz band, were reliably demodulated. These experiments were performed at environments and ranges that are being considered for underwater wireless networks.

After obtaining relatively poor results (high bit error rates) in the La Jolla data with an initial PPC-DPSK receiver

TABLE II. Bit error percentages from PPC-DPSK modulation at SignalEx F (off La Jolla in San Diego in 2002) for three bit rates at transmitter-receiver ranges of 500 m to 6.7 km. Each table entry represents four transmitted packets of 2240 bits each, corresponding to four receivers vertically separated by 14 in. (differences in bit error rate among the four receivers were negligible). Two packets, before and after the packet at 6.7 km, experienced some sort of recording failure, because no data was evident in the expected time interval (why the range increases by 1.2 km from 5.4 to 6.7, by twice the increment as for all the other packets, where the increment was roughly 0.6 km).

Range (km)	80 bps	160 bps	320 bps
0.6	0.00	0.16	16.20
1.2	0.00	0.10	17.98
1.8	0.04	0.85	26.81
2.4	0.00	0.34	13.84
3.1	0.00	0.04	10.84
3.7	0.06	3.07	29.35
4.3	0.16	6.96	31.30
4.9	0.14	10.01	35.37
5.4	0.07	4.08	26.01
6.7	0.23	9.64	36.53

design, we modified our receiver algorithm to omit low-amplitude contributions to the final phase comparison. At low amplitudes, most of the energy is due to sidelobes of the various correlation processes and to ambient noise. Restricting the phase comparison to higher amplitude contributions ensured that only those samples most likely to be multipath arrivals (and not spurious sidelobes) would contribute to the detection statistic. This is similar to what is sometimes done in Rake receivers for CDMA systems, where individual multipath arrivals are not included in the multipath recombination unless they exceed a minimum threshold. This modification resulted in greatly reducing the bit error rates at the 80 and 160 bps PPC-DPSK modulations. However, even with these improvements, the PPC-DPSK design at 320 bps consistently failed in the La Jolla test data. This was due to the level of multipath in this environment which exacerbated the degradation caused by compromises made to transmit at this rate, such as transmitting only part of the signal bandwidth needed to support the 16 kHz chip rate and clipping the signal to maintain its peak to average power ratio.

Thresholding the channel impulse response, so that only the strong arrivals contribute to the subsequent processing, can perhaps also improve the performance of other channel-estimate based signaling methods, including those based on multichannel time reversal (phase conjugation).

The novel modulation schemes considered in this paper have some interesting properties which may recommend them for use in operational systems. They are very simple, yet have a mechanism for dealing with intersymbol interference. Given their use of spread-spectrum sequences, they afford some potential for covert and multiuser applications. However, because their structure does not fully exploit the correlation properties of Gold sequences (due to multipath and because circular correlations cannot be used), they only mitigate intersymbol interference to a certain extent. As a result, the rates provided by these modulation schemes are relatively limited, compared to phase-coherent schemes in which more sophisticated receiver algorithms are typically used.

ACKNOWLEDGMENTS

SignalEx testing was sponsored by ONR 322OM (Tom Curtin and Al Benson). Additional support was provided by ONR 321OA. This work originated as part of the 6.2 Telesonar Technology program funded by ONR 321SS (Don Davison). We thank Joe Rice for originally suggesting this research.

[1]Stojanovic, M., Catipovic, J. A., and Proakis, J. G. (**1993**). "Adaptive multi-channel combining and equalization for underwater acoustic communications," J. Acoust. Soc. Am. **94**(3), 1621–1631.
[2]Stojanovic, M., Catipovic, J. A., and Proakis, J. G. (**1994**). "Phase-coherent digital communications for underwater acoustic channels," IEEE J. Ocean. Eng. **19**(1), 100–111.
[3]Parvulescu, A. (**1961**). "Signal detection in a multipath medium by M.E.S.S. processing," J. Acoust. Soc. Am. **33**(1), p. l674.
[4]Parvulescu, A. (**1995**). "Matched-signal (MESS) processing," J. Acoust. Soc. Am. **98**(2), 943–960.
[5]Parvulescu, A., and Clay, C. (**1965**). "Reproducibility of signal transmission in the ocean," Radio Electron. Eng. **29**, 223–228.
[6]Dowling, D. R. (**1994**). "Acoustic pulse compression using passive phase-conjugate processing," J. Acoust. Soc. Am. **95**(3), 1450–1458.
[7]Jackson, D. R., and Dowling, D. R. (**1991**). "Phase conjugation in underwater acoustics," J. Acoust. Soc. Am. **89**(1), 171–181.
[8]Kuperman, W. A., Hodgkiss, W. S., Song, H. C., Akal, T., Ferla, C., and Jackson, D. R. (**1998**). "Phase conjugation in the ocean: Experimental demonstration of an acoustic time-reversal mirror," J. Acoust. Soc. Am. **103**(1), 25–40.
[9]Edelmann, G. F., Akal, T., Hodgkiss, W. S., Kim, S., Kuperman, W. A., and Song, H. C. (**2002**). "An initial demonstration of underwater acoustic communication using time reversal," IEEE J. Ocean. Eng. **27**(3), 602–609.
[10]Rouseff, D., Jackson, D. R., Fox, W. L. J., Jones, C. D., Ritcey, J. A., and Dowling, D. (**2001**). "Underwater acoustic communication by passive-phase conjugation: Theory and experimental results," IEEE J. Ocean. Eng. **36**(4), 821–831.
[11]Rice, J., Creber, B., Fletcher, C., Baxley, P., Rogers, K., McDonald, V. K., Rees, D., Wolf, M., Merriam, S., Mehio, R., Proakis, J., Scussel, K., Porta, D., Baker, J., Hardiman, J., and Green, D. (**2000**). "Evolution of seaweb underwater acoustic networking," in *OCEANS, 2000. MTS/IEEE Conference Proceeding* (IEEE, Piscataway, N.J.), Vol. **3**, pp. 2007–2017.
[12]Hursky, P., Porter, M. B., Rice, J. A., and McDonald, V. K. (**2001**). "Passive phase-conjugate signaling using pulse-position modulation," in *OCEANS, 2001. MTS/IEEE Conference Proceedings* (IEEE, Piscataway, N.J), Vol. **4**, pp. 2244–2249.
[13]Flynn, J. A., Ritcey, J. A., Fox, W. L. J., Jackson, D. R., and Rouseff, D. (**2001**). "Decision-directed passive phase conjugation: equalisation performance in shallow water," Electron. Lett. **37**(25), 1551–1553.
[14]Peterson, R. L., Ziemer, R. E., and Borth, D. E. (**1995**). *Introduction to Spread Spectrum Communications* (Prentice-Hall, Upper Saddle River, NJ).
[15]Sarwater, D. V., and Pursley, M. B. (**1980**). "Crosscorrelation properties of pseudorandom and related sequences," Proc. IEEE **68**(5), 593–619.
[16]Dillard, G. M., Reuter, M., Zeiddler, J., and Zeidler, B., (**2003**). "Cyclic code shift keying: A low probability of intercept communication technique," IEEE Trans. Aerosp. Electron. Syst. **39**(3), 786–798.
[17]Ritcey, J. A., and Griep, K. R. (**1995**). "Code shift keyed spread spectrum for ocean acoustic telemetry," in *OCEANS, 1995. MTS/IEEE Conference Proceedings* 9–12 October in San Diego, CA (IEEE, Piscataway, N.J.) Vol. **3**, pp. 1386–1391.
[18]Sanchez, C., Koski, P., Brady, D., and Massa, D. (**1999**). "Sequence position modulation for surf-zone underwater acoustic communications," in *Proceedings of the 11th International Symposium on Unmanned Untethered Submersible Technology 23–25 August* (IEEE, Piscataway, N.J.), Vol. **11**, pp. 270–279.
[19]Proakis, J. (**2001**). *Digital Communications* (McGraw-Hill, NY).
[20]Yang, T. C. (**2003**). "Temporal resolutions of time-reversal and passive-

phase conjugation for underwater acoustic communications," IEEE J. Ocean. Eng. **28**(2), 229–245.
[21]Rouseff, D., Fox, W. L. J., Jackson, D. R., and Jones, C. D. (**2001**). "Underwater acoustic communication using passive phase conjugation," in *OCEANS, 2001. MTS/IEEE Conference Proceedings 5–8 November Honolulu, Hawaii* (IEEE, Piscataway, N.J.), Vol. **4**, pp. 2227–2230.
[22]Kwon, H. M., and Birdsall, T. G. (**1991**). "Digital waveform acoustic codings for ocean telemetry," IEEE J. Ocean. Eng. **16**(1), 56–65.
[23]Heard, G. J., and Schumacher, I. (**1996**). "Time compression of m-sequence transmissions in a very long waveguide with a moving source and receiver," J. Acoust. Soc. Am. **99**(6), 3431–3438.
[24]Sozer, E. M., Proakis, J. G., Stojanovic, M., Rice, J. A., Benson, A., and Hatch, M. (**1999**). "Direct sequence spread spectrum based modem for under water acoustic communication and channel measurements," in *OCEANS '99 MTS/IEEE. Riding the Crest into the 21st Century* (IEEE, Piscataway, N.J.), Vol. **1**, pp. 228–233.
[25]Porter, M. B., McDonald, V. K., Baxley, P. A., and Rice, J. A. (**2000**). "Signalex: linking environmental acoustics with the signaling schemes," in *OCEANS, 2000. MTS/IEEE Conference* (IEEE, Piscataway, N.J.), Vol. **1**, pp. 595–600.